

Low-temperature calorimetry on molecular glasses and crystals

Eloy Pérez-Enciso^a, Miguel A. Ramos^{b,*}

^a Tritón, Sistemas Experimentales, S.L., Felipe Moratilla 2, B, 28008 Madrid, Spain

^b LBT-UAM, Departamento de Física de la Materia Condensada C-III, Universidad Autónoma de Madrid, Cantoblanco, 28049 Madrid, Spain

Available online 10 May 2007

Abstract

We have designed and developed a versatile calorimetric system especially intended for glass-forming liquids, with which we are able to concurrently study and characterize the phase transitions in the range 77–300 K and also to measure their specific heat at low temperatures (0.3–30 K). At the former, higher temperatures we employ either a continuous method or the quasi-adiabatic, Nernst method. For specific-heat measurements at lower temperatures, we can use both quasi-adiabatic and thermal-relaxation methods. In particular, we have built up two complementary versions of the thermal-relaxation method (the standard one and an alternative version useful for longer relaxation times). A user-friendly PC software has been developed, allowing us to choose among the four calorimetric methods, as well as to tune all controlling parameters. We have applied this experimental system to investigate the calorimetric and thermodynamic behavior of the different solid phases of ethanol, as well as other interesting glass-forming systems such as alkyl-cyclohexanes or ionic liquids.

© 2007 Elsevier B.V. All rights reserved.

PACS: 65.60.+a; 65.40.Ba; 64.70.Dv; 07.20.Fw

Keywords: Specific heat; Thermal-relaxation calorimetry; Glass transition; Low-temperature properties of glasses; Molecular glasses and molecular crystals

1. Introduction

Although glass is a well-known and widely used material since thousands of years ago, the very nature of the glassy state and its physical properties remain an issue of vivid debate within the scientific community. Indeed, when some prominent scientists analyzed the main challenges to be addressed in the 21st century, it was stated that “*The deepest and most interesting unsolved problem in solid state theory is probably the theory of the nature of the glass and the glass transition*” [1]. In short, this major theoretical and phenomenological problem to be addressed has two prongs. One is related with the very nature of the glass transition: is it essentially a mere kinetic phenomenon or is there an underlying second-order thermodynamic transition [2–4]? The second prong is in the realm of solid-state physics and concerns the unexpectedly universal physical properties exhibited by glasses and other disordered solids at low-temperatures and/or low vibrational frequencies [5,6].

Thermal and calorimetric experiments are therefore most relevant for investigations in both of these fundamental aspects of the glass research. At relatively high temperatures, differential scanning calorimetry (DSC) is the most widely used thermoanalytical technique. Commercial DSC devices are often and efficiently employed above 100 K to observe and study a number of phase transitions in many different substances: crystallization and melting first-order transitions, glass transitions, polymorphism in food and pharmaceuticals, liquid crystalline transitions, etc. [7]. DSC is also frequently used for measurement of heat capacities, usually at relatively high scan rates, about 10–20 K/min. Since DSC measurements are dynamic, a calibration is usually carried out by using a standard sample with known heat capacity.

On the other hand, when cooling any material from room temperature to a few K, a tremendous reduction of thermal energy (say, by a factor of 10^4 to 10^7) occurs [8]. The technical difficulties arising from this drastic decrease in energy are the main problems which have prevented “low-temperature calorimeters” being commercially available. Therefore, measurements of the specific heat of solids at low-temperatures have always been a challenging task for low-temperature experimentalists. The first and easiest method to measure the specific heat of a material is

* Corresponding author. Tel.: +34 91 4975551; fax: +34 91 4973961.
E-mail address: miguel.ramos@uam.es (M.A. Ramos).

the adiabatic or Nernst calorimeter [8,9]. With this method, one directly determines the heat capacity per unit mass by accurately measuring the temperature increase produced in the sample after supplying a known amount of heat (i.e. a given electrical power during a fixed period of time). The need for excellent thermal isolation and the minimization of stray heat leaks makes however adiabatic calorimetry inapplicable in many cases. This has led to the development of several other calorimetric techniques [8,9], such as relaxation calorimetry, AC-temperature calorimetry or diffusive heat pulse calorimetry. Although much more technically complicated and time-consuming, these low-temperature techniques share the advantage of determining the specific heat of the sample in absolute terms, directly from a well-defined physical equation, in contrast to the calibration procedures required in commercial DSC.

Molecular liquids (at room temperature) have been and keep on being exhaustively studied by chemists and physicists. They also play a leading role in the research on glass-transition phenomena, since all relevant processes used to occur in the convenient temperature range between room and liquid-nitrogen temperatures. Three decades ago, Suga and Seki [10] studied exhaustively the thermodynamic behavior of a number of pure low-molecular weight compounds, by using three kinds of adiabatic calorimeters, more or less sophisticated, depending on the required cooling rates. They also employed a differential thermal analysis (DTA) apparatus to survey the general thermal behavior of a particular material prior to performing the quantitative measurements through adiabatic calorimetry. These authors found [10] glass-transition phenomena in all of the studied substances typically around $T \sim 100\text{--}200$ K. In some cases, they corresponded to standard glass transitions from the (amorphous) structural glass to the supercooled liquid (they called them *glassy liquids*); in other cases, the transitions were from an orientationally disordered crystal (ODC) – or “*glassy crystals*” – to its rotationally disordered plastic-crystalline phase. This dynamic transition from a non-ergodic state (the ODC phase) to an ergodic one (the plastic crystal, PC, which always has a small entropy of fusion and plays the role of the supercooled liquid) is therefore thermodynamically equivalent to the standard glass transition.

The most interesting case appeared to be ethanol ($\text{CH}_3\text{CH}_2\text{OH}$), which could be prepared [10–12] either as a stable (monoclinic) crystal, as a structural (amorphous) glass, or as a glassy crystal (i.e. an ODC) by quenching the PC phase, depending upon thermal histories and cooling rates below its melting point at $T_m = 159$ K. Very strikingly, both kinds of glass transitions (the canonical one and the dynamic PC–ODC transition) occur at the same temperature $T_g \approx 97$ K and with comparable jumps in specific heat. Ethanol thus appears as a good model system to investigate above-mentioned low-temperature properties of glasses [5,6], as well as the glass transition itself, discriminating the possible roles played by orientational and translational disorder. Indeed, we have shown [12,13] that both the structural (amorphous) glass and the orientational glass (i.e. a crystal with orientational disorder) phases of ethanol show, qualitatively and even quantitatively, the same glassy features in the low-temperature specific heat, altogether

with very similar glass-transition phenomena [10,14] between their corresponding ergodic and non-ergodic states.

During last years, we have been developing and improving a calorimetric experimental system appropriate to prepare and characterize *in situ* these different solid phases (from a sample which is originally liquid when mounted at room temperature), and then to measure their specific heat in a high-vacuum environment, both at low (liquid helium) cryogenic temperatures and intermediate (above liquid nitrogen) temperatures. In order to make further progress in this line of research, we have implemented higher-accuracy calorimetric methods (both quasi-adiabatic and thermal-relaxation ones) to measure low-temperature specific heat of different glassy and crystalline phases of different molecular compounds. Obviously, the employed methods and PC programs could be straightforward applied to measure the low-temperature specific heat of common samples of either crystals or glasses, that are already solid at room temperature. In addition, we have also implemented other calorimetric methods appropriate for higher temperatures in the transformation range of typical molecular glass-forming liquids, by developing a *quasi-adiabatic* continuous method which can be run in the same experimental set-up.

In the next sections, we will briefly describe this versatile calorimetric system and the different calorimetric methods that we can use for each situation, and provide a brief account of the developed software to conduct these calorimetric experiments. Some examples and tests of their use and applicability in our studied compounds will also be shown.

2. Experimental

2.1. Calorimetric set-up

The experimental set-up consists of a vacuum-tight copper cell, suspended by nylon threads from the inner flange of a cryostat. A silicon diode is used as thermometer in the higher temperature range and a commercially calibrated carbon resistor is usually employed at lower temperatures. A 1 k Ω resistor operates as electrical heater. These elements are glued onto the lower and upper surfaces of the cell. A simple, glass-dewar cryostat has been used, with a double-chamber insert to allow an independent thermal control of the reservoir temperature. Either liquid helium or liquid nitrogen is used, depending on the required temperature range. For temperatures below 2 K, a ^3He cryostat is employed instead [13]. Experiments were conducted in a high-vacuum environment ($\leq 10^{-7}$ mbar), supplying helium gas as thermal exchange gas when necessary.

In the present work, we have employed two kinds of calorimetric copper cells (see photo in Fig. 1). A first type of cell [11,15] is a copper cylindrical container (13 mm diameter, 25 mm height) with thin walls (< 0.5 mm), and with an indium sealed copper cover. Typical sample mass is here 2.5 g, for an empty copper cell of around 13 g. For some special compounds, aluminum was used [16] instead of copper to make the calorimetric cell. The second type of cell [12,13,17] was especially designed for measurements at low temperatures, as well as for allowing relatively high cooling rates to get a glass state. This



Fig. 1. Two main types of used calorimetric copper cells, compared to the size of an €1 coin.

cell is a small (approximately, 20 mm diameter, 5 mm height and very thin walls, 0.2 mm) pan-shaped, vacuum-tight copper container. In this case, typical sample mass is 1.5 g, for an empty copper cell of around 3 g. A fine copper mesh is fitted inside this sample holder to allow a rapid achievement of thermal equilibrium. Clean syringes were used for putting the liquid samples into the cells, which were immediately closed. For the latter, smaller copper cells, this is done by cutting and mechanically sealing the pre-soldered, appended tube. In all cases, a check for mass losses was performed after exposing the cell to dynamic vacuum from a diffusion pump. A second check on the total mass of the calorimetric cell, full of liquid, was performed at the end of each measurement run. All heat-capacity measurements, including those above 100 K to characterize the obtained phases, were carried out using the *same* experimental cell for a given substance. The latter was carefully weighted before and after being emptied. The heat capacity of one empty cell of each type was measured in order to subtract the addenda contribution. Small differences in weight (less than 5%) among different cells of the same kind were taken into account by considering the specific heat of copper. Measurements of a given material using different cells showed thus very good agreement and reproducibility.

2.2. Calorimetric methods

Three time scales are involved in a calorimetric measurement: the internal relaxation time τ_i of the energy inside the whole of the calorimetric cell (including sample, heater, thermometers and support), the relaxation time τ of the energy through the thermal contact (including all possible energy-loss channels), and the observation time interval during the experiment, τ_{exp} . Any calorimetric method here described assumes internal equilibrium states, so $\tau_i \ll \tau$.

If the same experimental set-up will be used for a wide temperature range, different calorimetric methods, each appropriate for a different temperature range, must be implemented. The different time scales determine the election of the different methods. In the range where different methods overlap, the reproducibility and accuracy of the whole set-up can be tested. Three *static* and one *dynamic* methods have been chosen and used within our system: quasi-adiabatic, standard relaxation, a

non-standard fast relaxation method, and an adapted continuous method.

The simplified form of the conduction equation relates a constant heating power P ($P = V_h I_h$, where V_h and I_h are the voltage drop in the heater element, and the electric current flowing through it, respectively) with the variation of energy in the cell and the energy losses through the thermal contact:

$$P = C_p(T) \frac{dT}{dt} + \int_{T_0}^{T_1} K_H(T) dT, \quad (1)$$

where we assume that the main energy loss occurs through the contact wire (a copper wire was chosen to have a relaxation time $\tau \sim 1$ min at liquid helium temperatures). If the heat capacity of the cell, C_p , is nearly constant for small temperature changes (typically $\Delta T/T \approx 1\%$), and the thermal conductance of the wire, K_H , is either linear or nearly constant for temperatures between the thermal reservoir temperature, T_0 , and the cell temperature, T_1 , the simplified form is thus:

$$P = C_p \frac{dT}{dt} + K_H \Delta T. \quad (2)$$

The solution for this linear differential equation is the well-known exponential expression:

$$\Delta T(t) = \frac{P}{K_H} \left[1 - \exp\left(-\frac{t}{\tau}\right) \right]; \quad \tau = \frac{C_p}{K_H}. \quad (3)$$

When the relaxation time τ is much larger than the typical time of the experiment, $\tau \gg \tau_{\text{exp}}$, the solution becomes the usual adiabatic case:

$$\Delta T(t) \approx \frac{P}{K_H} \left[1 - \left(1 - \frac{t}{\tau}\right) \right] = \frac{P}{C_p} t \Rightarrow C_p = \frac{P \Delta t}{\Delta T}, \quad (4)$$

where Δt is the fixed time for heating the cell at power P . In this adiabatic solution, as the time required to cool the sample is extremely large, the temperature remains constant when no power is applied. (In a more realistic, *quasi-adiabatic* case, a small thermal drift is observed. This can be easily subtracted [8] from the temperature recording, by making least-squares linear fittings for the drift curves $T_0(t)$, both before and after the heating period, provided they keep reasonably parallel). A non-zero heating power will increase linearly the cell temperature. On the other hand, when τ is closer to τ_{exp} , the observed temperature variations are no longer linear but exponential, i.e. relaxations of energy.

Nevertheless, in order to measure heat capacity C_p at low-temperatures, relaxation calorimetry is often used instead of adiabatic calorimetry, since it is more suitable for smaller samples and/or lower temperatures, and avoids the requirements of perfect adiabaticity. In the first part of the standard relaxation method [9,18], one waits until the steady-state equilibrium between the heating and cooling power is achieved. At this point, the increase in temperature remains constant: $\Delta T_\infty = P/K_H$. In the second part, the heating power is switched off and the relaxation of temperature is recorded:

$$T(t) = T_0(t) + \Delta T_\infty \exp\left(-\frac{t}{\tau}\right). \quad (5)$$

The linear fitting of the exponential decay in a semi-log plot gives the time constant τ , the thermal conductance parameter is directly $K_H = P/\Delta T_\infty$, and hence the value of the heat capacity is obtained

$$C_p = K_H \tau. \quad (6)$$

However, when the relaxation times to equilibrium, τ and therefore τ_{exp} , are getting larger (typically with increasing temperature), some inaccuracies could appear in a real experiment, mainly due to variations on the reference temperature $T_0(t)$. A faster relaxation method can then be used, in which the steady-state heating equilibrium is not reached. The key idea is to make also use of the heating part of the recorded data, by fitting it to Eq. (3). As τ is known from the cooling-curve fit, after a simple variable change, $t \rightarrow \delta = [1 - \exp(-t/\tau)]$, and the heating equation becomes $\Delta T(\delta) = (P/K_H)\delta$. Thus, a simple least-squares linear fit provides the missing parameter K_H , and the heat capacity is again obtained from Eq. (6). In the low-temperature experiments shown in this work, K_H ranged typically between 20 and 100 $\mu\text{W/K}$. The goodness of these exponential fits will depend on the goodness of the condition $\tau_i \ll \tau$ and on having a well-defined thermal link. By using this non-standard relaxation method the total experiment time can be reduced dramatically, and hence the accuracy is improved, since one avoids a large error coming from a non-stable reference temperature $T_0(t)$.

For measurements above 77 K, specific heat was measured by means of a quasi-adiabatic, continuous method. Even if apparently adiabatic, any calorimetric cell is in contact with the thermal reservoir at 77 K through an effective thermal link (mainly arising from blackbody thermal radiation plus conduction through the electrical wiring). Therefore, the equation of heat transport contains both a cooling P_{cool} and a heating P_{heat} power terms, so that

$$C_p \left(\frac{dT}{dt} \right) = P_{\text{heat}} + P_{\text{cool}} = V_h I_h + C_p \Theta(T), \quad (7)$$

where $\Theta(T) \equiv (dT/dt)_{\text{drift}}$ is the intrinsic (negative) thermal drift of the system, which is directly measured as a function of temperature by standard cooling at $I_h = 0$, with the thermal reservoir fixed at 77 K. These measurements should be done independently for each phase of the studied substance, since differences in their specific heat imply (slightly) different thermal drift $\Theta(T)$ curves for the whole system. Then, the heat capacity can be determined from

$$C_p = \frac{V_h I_h}{dT/dt - \Theta(T)}. \quad (8)$$

Finally, the heat capacity of the empty cell is measured separately, so that its contribution can be subtracted and the wanted specific heat data of the sample obtained.

On the other hand, a direct display of the measured dT/dt curve as a function of temperature T , for a constant applied power, is besides a useful thermogram to monitor first-order transitions such as melting and crystallization processes (see, for instance, Refs. [11,14–16]).

With this experimental system, maximum cooling rates attainable are around -20 K min^{-1} , using the second type of

cell, and heating rates should be below $+4 \text{ K min}^{-1}$ to obtain reliable results in absolute terms, whereas there is no limitation to conduct cooling or heating processes as slow as desired.

2.3. PC software for calorimetry

An application, “LBT Calorimetría”, was developed for the automation of the calorimetric methods, user selection of all control parameters, and data analysis. It was developed in the framework of Borland BDS 2006[®]. The application is composed of different functional modules: heat capacity, thermal conductivity, thermal expansion, and other modules for the data analysis, and automation of temperature controllers. So, a wide thermal characterization of the system can be done. Different thermal properties could even be measured at the same time for the same sample.

The power applied by the heaters and the temperature reading by the thermometers are nothing else than voltage and current measurements, so the user can choose between a wide series of precision current sources and high-sensitivity voltmeters. Accuracy thermometry is a must in these experiments, and hence well-calibrated thermometers are used. Due to the wide temperature range of interest, several kind of thermometers and calibration curves can be selected within the program by the user. Different types of calibration files can be imported, either as polynomial fits (Chebyshev, power series, logarithmic, inverse power series, etc) or calibration data to be interpolated. At any time, the current in the resistance thermometers is automatically set, so that the voltage drop is a user selectable value (typically a few millivolts). Current polarity is also changed to avoid thermoelectric offset.

In addition, the user can choose among several temperature controllers for temperature stabilization or ramping of cryostat chambers.

Once the heat capacity module has been launched and the instrumentation and thermometry has been selected, the user must choose the measurement method, modify any of the measurement parameters, and start the run. After one heat-capacity data point at a given temperature has been obtained, the program automatically changes the chamber temperature to a user-selectable amount. When the conditions for a new run are given, a new heat-capacity measurement is started. The whole routine ends either by a user order or by a high-temperature security condition.

For a high versatility of the program, the new run condition is fired either by a user order, when a user selectable time has elapsed, when the base temperature has changed by a user selectable value, or when the equilibrium to the new temperature is achieved. This is programmatically implemented by a temperature slope smaller than a given value.

Although small in terms of temperature slope, there is always a thermal drift which is recorded during the first part of the run. As the heat capacity of the cell is known from the last run, the program automatically determines the heating power to obtain the selected porcentual increase in temperature, in a given heating time which is also pre-selected by the user. In all cases, the running $T(t)$ curve is being displayed on the screen,

together with all the relevant information about the currently selected items, variables or controlling parameters.

In the quasi-adiabatic case, the thermal drift after heating is recorded. The run stop condition is fired by a user order, when the slope is similar enough to the initial one by a user selectable parameter, or when a user selectable value elapsed. Effective temperature increase is calculated by extrapolation of drifts to the midpoint of heating time.

In the standard relaxation method, heating is stopped when the slope is similar enough to the initial one, and ΔT_∞ is now obtained by extrapolation of the slopes to the end of heating time. The program will fit the relaxation curve for the data between upper and lower limits. Those limits are selected as percentual values of ΔT_∞ , typically 5% and 80%. Good exponential fits are obtained only if the extrapolated drift of the first part of the run is subtracted from the recorded data. This is also true for the fits in both the heating and cooling parts of the fast relaxation method. Moreover, the program opens graphic windows on the screen to show instantaneously the semilogarithmic plots of the running experiment, and the corresponding linear fits, to monitor the good thermal behavior of the experiment.

Finally, the continuous method is run by simply recording the temperature reading of the thermometer(s) as a function of time $T(t)$, also recording the instantaneous voltage drop in the heater and any other required parameters. Specific-heat curves are obtained in a subsequent data analysis by using Eq. (8).

3. Results and discussion

In this section, we will present some direct examples of experimental data obtained with our calorimetric system. In all cases to be presented here, the studied sample is pure ethanol, in some of its different phases. One example of an experimental point obtained by the classical adiabatic method for the orientationally disordered crystal (ODC) phase of ethanol is depicted in Fig. 2. For a pre-selected temperature increase, $\Delta T/T \approx 1\%$, the program estimates the required power, which is applied for a given period of time Δt . The average temperature of the measurement (82.3 K in this case) is obviously given by the midpoint of the produced temperature jump ΔT . P_1 and P_2 indicate the automat-

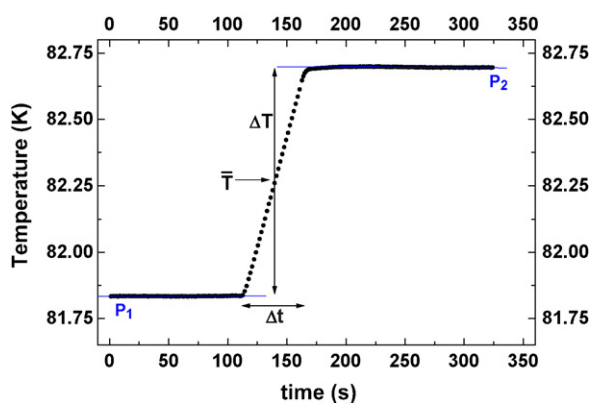


Fig. 2. Example of adiabatic point, taken at 82.3 K (the midpoint of the jump) in the orientationally disordered crystal (ODC) phase of ethanol. P_1 and P_2 indicate the linear fits for the thermal drift before and after the heating step, respectively.

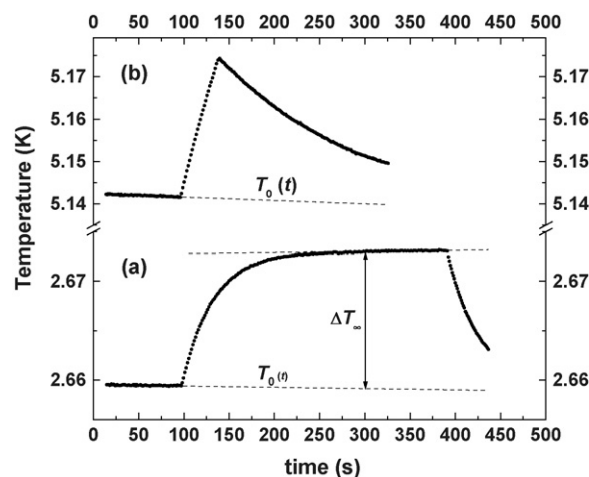


Fig. 3. Examples of experimental points obtained for glassy ethanol at low temperatures, using the standard relaxation method (a) and the alternative fast relaxation method (b), as explained in the text. The thermal drift curves $T_0(t)$ are indicated with dashed lines.

ically fitted linear backgrounds for the thermal drift before and after the heating step, respectively. When these are long and parallel enough, the point is completed and a new point is started. The heat capacity of the calorimetric cell at the above-mentioned average temperature is then straightforward determined by Eq. (4).

As reminded in the previous section, in the standard thermal-relaxation method (see Fig. 3a), the temperature T of the sample is raised (by around 1%) and then let to decay exponentially with time t , following Eq. (5). On the other hand, when the relaxation time τ is getting longer (this typically happens with increasing temperature), we can replace the long-time heating step by a shorter heating curve (see Fig. 3b), that follows Eq. (3). In this alternative, two-step relaxation method, ΔT_∞ is not measured directly, but determined from a simple linear fit (see inset in Fig. 4) of the heating curve $\Delta t(\delta) = (P/K_H)\delta$ defined above, after having determined τ from the cooling relaxational curve by Eq. (5). As can be seen in Fig. 4, the excellent linear behavior of the semilogarithmic plots in both cases guarantees the existence of

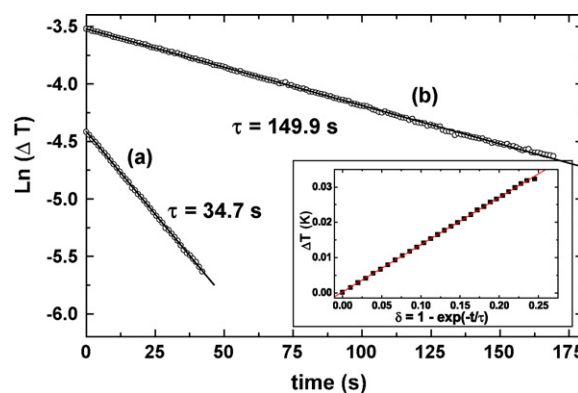


Fig. 4. Examples of the semilogarithmic plots from Eq. (5) used to determine the time constant τ for the experimental data of Fig. 3. Inset: linear fit to the heating curve for the fast relaxation method (b), $\Delta T(\delta) = (P/K_H)\delta$, where $\delta = [1 - \exp(-t/\tau)]\delta$; see Eq. (3) in the text.

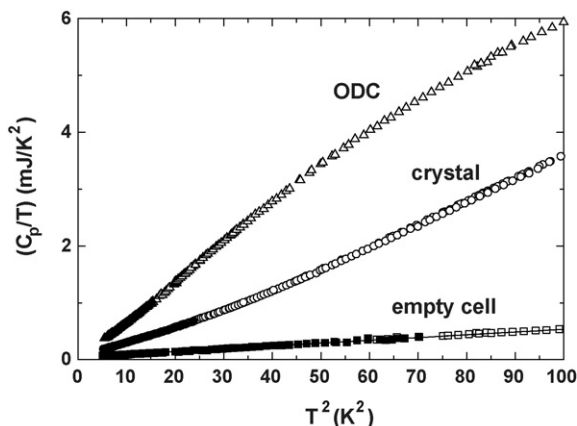


Fig. 5. Total low-temperature heat-capacity in a C_p/T vs. T^2 plot, measured for pure ethanol, in ODC (triangles) and crystal (circles) phases, as well as the heat capacity measured for the empty cell (squares) in order to be subtracted. Solid symbols correspond to data measured by the standard relaxation method and open symbols by the alternative fast relaxation method (see text for more details).

a well-defined relaxation time τ for the effective thermal link and improves the accuracy of the measurement.

In Fig. 5, we present heat-capacity data in a C_p/T versus T^2 plot obtained at low temperatures for different phases of pure ethanol, together with the measurement of the empty cell. After subtracting the latter and dividing by the corresponding amount of ethanol in each case, the desired molar specific heat can be determined. As can be observed there, data obtained from either the standard relaxation method (curve (a) in Fig. 3) or from the alternative one (curve (b) in Fig. 3) agree very well with each other.

Finally, we show in Fig. 6 several specific-heat curves obtained [14] for pure ethanol across the dynamic glass-transition ODC \rightarrow PC, as well as for the stable, monoclinic crystal phase and its melting transition into the liquid state. These data are obtained from measured dT/dt curves (typically

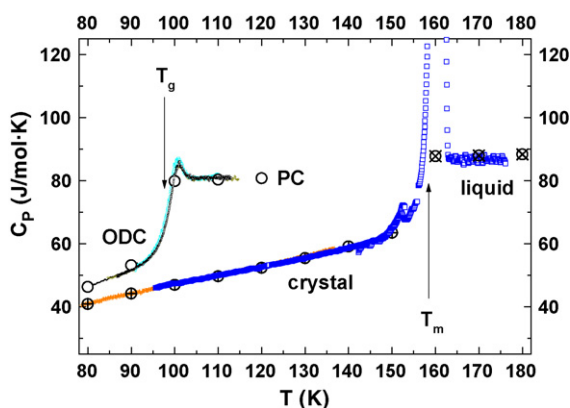


Fig. 6. Molar specific heat of ODC–PC phases (upper curves) and monoclinic crystalline phases of pure ethanol. Different (almost indistinguishable) shown solid curves (ODC–PC) and symbols (crystal) correspond to different experimental runs. Measurements were conducted by heating at approximately $+1 \text{ K min}^{-1}$. Different shown ODC phases were obtained after cooling rates between -2 and -6 K min^{-1} . Big circles are adiabatic data from the literature [10] for the corresponding phases.

using heating rates around 1 K min^{-1}), following the procedure described at the end of Section 2.2. All measurements shown in Figs. 2–6 have been performed using the smaller and thinner kind of copper cell (see Fig. 1), which is especially appropriate for lower temperatures. Nevertheless, calorimetric experiments at temperatures above 77 K have also been successfully conducted with the larger cylindrical cells, made of either copper or aluminium. Experiments with these cells have been reported for ethanol [11], alkyl-cyclohexanes [15], and ionic liquids [16]. A fair agreement of data obtained with both types of calorimetric cells, using the adiabatic method, can be seen in Fig. 2 of Ref. [11]. However, to calorimetrically study molecular glass-forming liquids in this temperature range, our adapted continuous method seems to be the most accurate and advantageous. Its reproducibility and precision can be assessed in Fig. 6, where different experimental runs taken in different days, with (slightly) different conditions, provide almost indistinguishable results in absolute terms (see more of these reproducible $C_p(T)$ curves in Figs. 3 and 4 of Ref. [14]). Furthermore, our molar specific-heat data are in excellent agreement with earlier data from the literature [10], that were obtained with the standard adiabatic method.

4. Conclusions

We have presented a versatile experimental program for calorimetric measurements. It allows to tune adiabatic or continuous methods to monitor and characterize phase transitions at higher temperatures, and also two alternative thermal-relaxation methods for low-temperature specific-heat measurements, the latter depending on the value of the time constant which usually increases with temperature. Calorimetric set-ups especially developed for studying molecular glass-forming liquids have also been briefly described. A sample of experiments conducted with this calorimetric program on different phases of ethanol, both in liquid-helium and liquid-nitrogen cryogenic environments, have been shown. In the present article, special emphasis has been put on describing the different calorimetric methods available within it (some better known and more often used, other relatively new adaptations), as well as the accuracy and reproducibility achieved. This accuracy is nonetheless compatible with a convenient, reasonably fast (up to a few K min^{-1}) performance to study *in situ* the phase transitions of the same substance and cell which is to be measured at very low temperatures.

Acknowledgements

We thank Dr. J.G. Rodrigo for his contribution in programming the continuous method. We acknowledge financial support by the Spanish Ministry of Education and Science within project FIS2006-01117, and from the Comunidad de Madrid within “CiTecnoMiK” program (S-0505/ESP/0337).

References

- [1] P.W. Anderson, *Science* 267 (1995) 1615–1616.
- [2] I. Gutzow, J. Schmelzer, *The Vitreous State*, Springer, Berlin, 1995.

- [3] P.G. Debenedetti, *Metastable Liquids: Concepts and Principles*, Princeton University Press, Princeton, 1996.
- [4] K. Binder, W. Kob, *Glassy Materials and Disordered Solids*, World Scientific, Singapore, 2005.
- [5] W.A. Phillips (Ed.), *Amorphous Solids: Low Temperature Properties*, Springer, Berlin, 1981.
- [6] P. Esquinazi (Ed.), *Tunnelling Systems in Amorphous and Crystalline Solids*, Springer, Berlin, 1998.
- [7] G.W.H. Höhne, W. Hemminger, H.J. Flammersheim, *Differential Scanning Calorimetry*, Springer, Berlin, 1996.
- [8] E. Gmelin, *Thermochim. Acta* 29 (1979) 1–39.
- [9] T.H.K. Barron, G.K. White, *Heat Capacity Thermal Expansion at Low Temperatures*, Kluwer, New York, 1999.
- [10] H. Suga, S. Seki, *J. Non-Cryst. Solids* 16 (1974) 171–194;
O. Haida, H. Suga, S. Seki, *J. Chem. Thermodyn.* 9 (1977) 1133–1148.
- [11] M.A. Ramos, I.M. Shmyt'ko, E.A. Arnautova, R.J. Jiménez-Riobóo, V. Rodríguez-Mora, S. Vieira, M.J. Capitán, *J. Non-Cryst. Solids* 352 (2006) 4769–4775.
- [12] M.A. Ramos, C. Talón, R.J. Jiménez-Riobóo, S. Vieira, *J. Phys.: Condens. Matter* 15 (2003) S1007–S1018.
- [13] C. Talón, M.A. Ramos, S. Vieira, *Phys. Rev. B* 66 (2002) 012201.
- [14] M.A. Ramos, V. Rodríguez-Mora, R.J. Jiménez-Riobóo, *J. Phys.: Condens. Matter* 19 (2007) 205135.
- [15] A. Mandanici, M. Cutroni, A. Triolo, V. Rodríguez-Mora, M.A. Ramos, *J. Chem. Phys.* 125 (2006) 054514.
- [16] A. Triolo, A. Mandanici, O. Russina, V. Rodríguez-Mora, M. Cutroni, C. Hardacre, M. Nieuwenhuyzen, H.J. Bleif, L. Keller, M.A. Ramos, *J. Phys. Chem. B* 110 (2006) 21357–21364.
- [17] C. Talón, M.A. Ramos, S. Vieira, G.J. Cuello, F.J. Bermejo, A. Criado, M.L. Senent, S.M. Bennington, H.E. Fischer, H. Schober, *Phys. Rev. B* 58 (1998) 745–755.
- [18] R. Bachmann, F.J. DiSalvo Jr., T.H. Geballe, R.L. Greene, R.E. Howard, C.N. King, H.C. Kirsch, K.N. Lee, R.E. Schwall, H.U. Thomas, R.B. Zubeck, *Rev. Sci. Instrum.* 43 (1972) 205–213.